JOURNAL OF GUIDANCE, CONTROL, AND DYNAMICS
Vol. 20, No. 3, May–June 1997

Conflict Probability Estimation for Free Flight

Russell A. Paielli and Heinz Erzberger
NASA Ames Research Center, Moffett Field, California 94035-1000

The safety and efficiency of free flight will benefit from automated conflict prediction and resolution advisories. Conflict prediction is based on trajectory prediction and is less certain the farther in advance the prediction, however. An estimate is needed, therefore, of the probability that a conflict will occur, given a pair of predicted trajectories and their levels of uncertainty. A method to estimate that conflict probability is presented. The trajectory prediction errors are modeled as normally distributed, and the two error covariances for an aircraft pair are combined into a single, equivalent covariance of the relative position. A coordinate transformation is then used to derive an analytical solution. Numerical examples and a Monte Carlo validation are presented.

Introduction

THE economics and efficiency of air transportation in the continental United States could be improved significantly if the rigid routing restrictions[1] currently imposed by the Federal Aviation Administration were relaxed to allow more direct or wind-optimal trajectories. The current routing restrictions help to maintain the safe and orderly flow of traffic, but new technologies in the areas of tracking, prediction, and communication are being developed that can be used to maintain or improve safety while relaxing or eliminating those restrictions. The ultimate goal is free flight,[2–4] which could save the airlines several billion dollars per year in direct operating costs, according to the Air Transport Association. The safety and efficiency of free flight will benefit from automated conflict predictions and resolution advisories. By definition, a conflict (not to be confused with a collision) occurs when two or more aircraft come within the minimum allowed distance between each other. The minimum allowed horizontal separation for en-route airspace is currently 5 n miles. The vertical separation requirement above an altitude of 29,000 ft is currently 2000 ft; below that level it is 1000 ft.

Aircraft trajectory prediction is inexact, primarily because of wind modeling and prediction errors and secondarily because of tracking, navigation, and control errors. Wind estimates, based on the mesoscale analysis and prediction system rapid update cycle,[5,6] are provided by the National Oceanic and Atmospheric Administration. Aircraft in cruise are usually programmed to stay on track laterally and vertically and to maintain a particular airspeed or Mach number. The farther in advance trajectories are predicted, the more uncertain those predictions are, particularly in the along-track direction, because the resulting ground speed depends on the winds, and the uncompensated effects of wind errors accumulate over time. Because conflict prediction is based on trajectory prediction, the farther in advance a potential conflict is predicted to occur or not to occur, the less certain that the prediction is likely to be. A method is needed to estimate the level of certainty.

The optimal time to initiate a conflict resolution maneuver is a tradeoff between efficiency and certainty. The farther in advance a maneuver is initiated, the more efficient it is likely to be in terms of extra distance flown, but the less certain will be exactly what maneuver is required or whether a maneuver is required at all. The later a maneuver is initiated, on the other hand, the more certain will be exactly what maneuver is required, but the less efficient and more harsh the maneuver is likely to be. The determination of the optimal time to initiate a maneuver, therefore, requires an estimate of conflict probability.

The determination of the optimal maneuver to be executed also requires a method of estimating conflict probability because the goal of conflict resolution is to reduce the postresolution conflict probability to some acceptable level. The conflict probability cannot be reduced to zero without introducing gross inefficiency, but that is not necessary because human air traffic controllers will be available to catch any unresolved conflicts. The methods presented in this paper are intended to assist rather than replace human air

Russell A. Paielli received his B.S. degree in mechanical engineering from Oakland University in Michigan in 1982 and has worked at NASA Ames Research Center since then. He received his M.S. degree in aeronautics and astronautics from Stanford University in 1987. At NASA Ames Research Center he has done research in flight control theory and precision aircraft navigation and landing. He is currently in the Flight Management and Human Factors Division at NASA Ames Research Center and is working on conflict prediction and resolution for free flight. He is a Senior Member of AIAA.

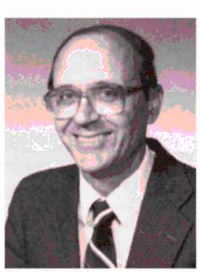

Heinz Erzberger is the senior scientist for air traffic management at NASA Ames Research Center. He has been with NASA Ames Research Center since receiving his Ph.D. degree in electrical engineering from Cornell University. His research has focused on aircraft trajectory optimization, four-dimensional guidance, and concepts for automated air traffic control. His honors and awards include the NASA Outstanding Leadership Medal, the Theodore von Kármán Lectureship Award of Israel, and the AIAA Mechanics and Control of Flight Award. He is the chief designer of the Center–Tracon Automation System, which the Federal Aviation Administration is now installing at high-density airports and air traffic control facilities. He was the recipient of the 1997 AIAA Dryden Lectureship for Research, and the content of the current paper composed a portion of his Dryden Lecture. He is a Fellow of AIAA.

Received July 18, 1996; revision received Nov. 26, 1996; accepted for publication Nov. 29, 1996.

traffic controllers. That is, they are intended to provide automated advisories for the controllers but not to make the ultimate decisions.

A method is developed in this paper to estimate the conflict probability for a pair of aircraft in free flight. The trajectory prediction errors are modeled as normally distributed, and the two error covariances for an aircraft pair are combined into a single, equivalent covariance of the relative position. A coordinate transformation is used to derive an analytical solution. The paper is organized as follows. First, some background is given on modeling of trajectory prediction errors and conflict prediction. The conflict probability estimation algorithm is then developed. Finally, some numerical examples and a Monte Carlo validation are presented.

Conflict Prediction

Conflict prediction can be divided into the following three steps. First, the trajectories of all aircraft in the region of interest are predicted for approximately the next 20–30 min. These deterministic predictions are based on current estimated positions and velocities, flight plans, and predicted winds aloft. This complex modeling and software problem has already been solved for arrival traffic as part of the Center–Tracon automation system (CTAS),[7] and that solution will be adapted for en-route and departure traffic also. The second step is to coarsely screen all possible aircraft pairs to eliminate those with a negligible possibility of conflict. The third step, which is the subject of this paper, is to estimate the conflict probability for those remaining aircraft pairs. This probability involves the predicted trajectories and an estimate of their uncertainty.

The lateral feedback loop is typically closed around cross-track position either by the pilot or by a flight management system (FMS). The stabilized cross-track rms prediction error is approximately constant, with typical magnitudes from less than 0.5 n mile for aircraft equipped with an FMS to more than 1 n mile for those without. This magnitude also could be a function of the crosswind magnitude.

Longitudinal position control involves using the throttle to compensate for unpredictable variations in headwinds or tailwinds. Because such compensation tends to be inefficient in cruise, the longitudinal feedback loop is usually closed around Mach number or airspeed but not ground speed or along-track position. For trajectory predictions of up to 20 or 30 min, the unstabilized along-track rms error tends to grow approximately linearly, as illustrated in Fig. 1, with a typical growth rate of 0.25 n mile/min (15 kn) in cruise. This growth rate is primarily due to wind-prediction bias error, and it could be reduced in the future with improved wind modeling or with low-bandwidth control of along-track position, if such control can be done efficiently enough.

The vertical rms error is primarily due to baroaltimeter error and secondarily due to altitude control error. The vertical error and along-track rms prediction error growth rate are both greater in climb and descent than in cruise. For predictions involving more than one flight regime (such as climb and cruise, for example) the total rms error is the sum of the contributions from each segment. Turns also tend to be imprecise and, therefore, add a significant amount of uncertainty that should be accounted for.

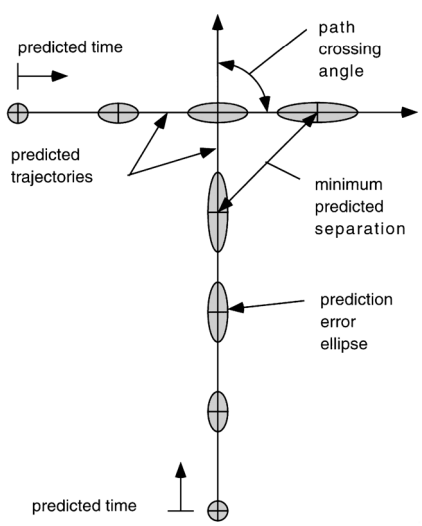

Fig. 1 Trajectory prediction error ellipses.

For the purposes of this paper, the magnitudes of the rms prediction errors and their growth rates are merely parameters. What is important is that the prediction errors can be approximated as normally distributed (Gaussian) because the algorithm to be presented in this paper is based on that model. Many other estimation algorithms, such as the classic Kalman filter, are also based on the normal distribution model. Ballin and Erzberger[8] tested the accuracy of the trajectory-prediction software that is installed in the Fort Worth Air Route Traffic Control Center as part of CTAS. They analyzed data from cruise segments of over 4000 flights (eliminating those with delays that could be caused by unscheduled maneuvers) and found that the along-track prediction errors were indeed very close to normally distributed.

The normally distributed prediction errors can be represented as ellipses in the horizontal plane or as ellipsoids in space. The error ellipses tend to have their major principal axis in the along-track direction and their minor principal axis in the cross-track direction. [Note that the uncertainty ellipse for normally distributed random variable x is defined as the solution of $z^T Z^{-1} z = c^2$, where $z = x - E(x)$, $Z = \text{cov}(z) \equiv E(zz^T)$, E is the expected value, and c is a constant that can be assumed to be unity unless otherwise noted.]

The cross correlation of prediction errors between aircraft can also be important because common errors cancel in the position difference or relative position. Unfortunately, the cross correlation is more difficult to model than the individual covariances because it depends on the trajectories and a spatial wind-error correlation model. That correlation model will be a function of both separation distance and heading angular difference. Aircraft pairs with nearly perpendicular flight paths will tend to have weakly cross-correlated prediction errors because their along-track positions are affected by different wind components. Aircraft pairs with small path-crossing angles (and small minimum separations), on the other hand, will tend to have more strongly cross-correlated prediction errors both because they are affected by a common wind component and because they spend a relatively long time close together. Although this area is open for research, it is not pursued in this paper.

Conflict Probability Estimation

This section is divided into five subsections. First, the method of combining two prediction-error covariances into a single covariance of the relative position is discussed. Next, a coordinate transformation is proposed that transforms the combined error covariance into a standard form. Then the analytical solution for the conflict probability in two dimensions is developed. The generalization from two to three dimensions is then discussed. Finally, the application to conflict resolution is previewed.

Combined Error Covariance

The trajectory prediction error for an aircraft will be modeled as normally distributed, with zero mean and with a covariance that has eigenvectors in the along-track and cross-track directions, as explained previously. The covariance matrix is therefore diagonal in a coordinate system aligned with the aircraft heading. If q is the aircraft position in such a heading-aligned coordinate system, and $\bar{q}$ is the corresponding prediction, then the prediction error is

$$\tilde{q} \equiv q - \bar{q} \tag{1}$$

and the corresponding diagonal covariance matrix is

$$S \equiv \text{cov}(\tilde{q}) \tag{2}$$

where $\text{cov}(x) \equiv E(xx^T)$ for any random variable x and E is the expected value function. If ψ is the heading angle in some Earth-fixed reference coordinate system, then

$$R \equiv \begin{bmatrix} \cos\psi & -\sin\psi \\ \sin\psi & \cos\psi \end{bmatrix} \tag{3}$$

is a rotation matrix that transforms the heading-aligned coordinates to the reference coordinates. The position prediction in the reference coordinate system is then

$$\bar{p} = R\bar{q} \tag{4}$$

The position prediction error is

$$\tilde{p} = R\tilde{q} \tag{5}$$

and the corresponding covariance matrix is

$$Q \equiv \text{cov}(\tilde{p}) = RSR^T \tag{6}$$

Because the trajectory prediction errors are modeled as normally distributed, the two error covariances for an aircraft pair can be easily combined into a single equivalent covariance of the position difference or the relative position of one aircraft with respect to the other. For the present purposes, this combined covariance can be assigned to one of the aircraft, referred to as the stochastic aircraft, and the other aircraft, referred to as the reference aircraft, can be regarded as having no position uncertainty.

Let subscripts S and R designate the stochastic and reference aircraft, respectively. The position difference is

$$\Delta p \equiv p_S - p_R \tag{7}$$

The prediction of that position difference is

$$\Delta \bar{p} \equiv \bar{p}_S - \bar{p}_R \tag{8}$$

and the prediction error is

$$\Delta \tilde{p} \equiv \Delta p - \Delta \bar{p} = \tilde{p}_S - \tilde{p}_R \tag{9}$$

The combined prediction error covariance is then

$$M \equiv \text{cov}(\Delta \tilde{p}) = Q_S + Q_R - Q_{SR} \tag{10}$$

where Q_S and Q_R are the individual covariances based on Eq. (6) and the cross-correlation term Q_{SR} is defined as

$$Q_{SR} \equiv E\left(\tilde{p}_S \tilde{p}_R^T + \tilde{p}_R \tilde{p}_S^T\right) \tag{11}$$

In general, the combined error ellipse corresponding to M will no longer have principal axes aligned with the along-track and cross-track directions of either aircraft.

Figure 2 shows an example of encounter geometry, with the combined error ellipse centered on the stochastic aircraft and the circular conflict zone (5-n mile radius) centered on the reference aircraft. The error ellipse corresponds to a probability density function that can be represented as a surface over the ellipse. The ellipse is actually the intersection of that surface and a horizontal plane cutting the surface. The total volume under the surface is unity. The probability of conflict at a particular time is the portion of that volume that is within the circular conflict zone. An analytical solution has not been found for this probability, but it is not as important as the total probability of conflict for the encounter, which is discussed in the following paragraphs.

It is assumed that the aircraft velocities and prediction errors are constant during the encounter or period of potential conflict, which is at least approximately true for most aircraft pairs in free flight. The total probability of conflict for the encounter can then be determined as follows. Project the circular conflict zone along a line parallel to the relative velocity to form an extended conflict zone, as illustrated in Fig. 2. The conflict probability is equal to the portion of the volume under the probability density surface that is within this extended conflict zone. The coordinate transformation to be presented in the next section allows this probability to be determined analytically.

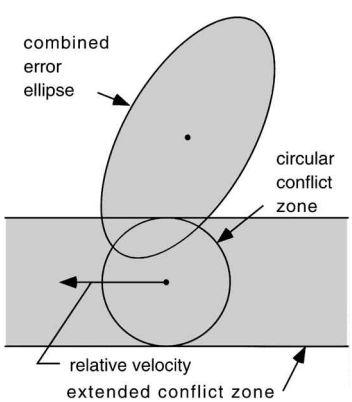

Fig. 2 Encounter geometry.

Coordinate Transformation

Coordinate transformations are often useful for simplifying problems. They are widely used in control theory, for example. In this case, the conflict probability is difficult or impossible to determine analytically in the original coordinate system. It can be determined numerically, but a numerical solution is likely to be much less efficient and less accurate than an analytical solution. This inefficiency is undesirable for an algorithm that is intended to run in real time at a very high rate for many years. Fortunately, a coordinate transformation has been found that allows an analytical solution.

Let p and ρ represent the original and transformed coordinates of position, respectively. A general linear coordinate transformation is of the form

$$\rho = Tp \tag{12}$$

$$p = W\rho \tag{13}$$

where T is a transformation matrix to be determined and $W \equiv T^{-1}$. The transformations for velocity and other vectors are of the same form. Combining the definition

$$\Delta \rho \equiv \rho_S - \rho_R \tag{14}$$

with the definitions in Eqs. (7–9) gives

$$\Delta \tilde{\rho} = T\Delta \tilde{p} \tag{15}$$

In the transformed coordinate system, the mean prediction error is still zero and the combined error covariance is

$$\text{cov}(\Delta \tilde{\rho}) = TMT^T \tag{16}$$

where $M \equiv \text{cov}(\Delta \tilde{p})$ is the combined error covariance in the original coordinate system from Eq. (10).

A Cholesky decomposition[9] or "square-root" factorization of the combined error covariance M is of the form

$$M = LL^T \tag{17}$$

where L is lower triangular. If T is of the form

$$T = RL^{-1} \tag{18}$$

where R is any orthogonal rotation matrix, then Eq. (16) becomes

$$\text{cov}(\Delta \tilde{\rho}) = I \tag{19}$$

where the fact that $RR^T = I$ has been used. The combined error ellipse is therefore in the standard form of a unit circle, as shown in Fig. 3. The conflict boundary, which was a circle in the original coordinate system, is an ellipse in the transformed coordinate system, also as shown in Fig. 3.

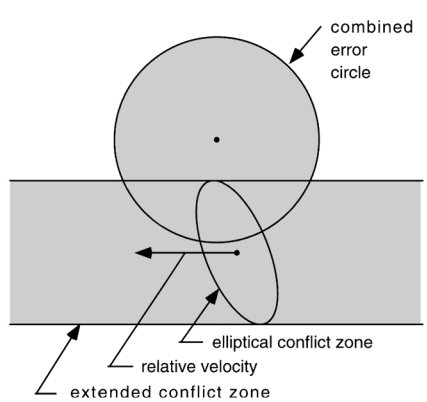

Fig. 3 Transformed encounter geometry.

Analytical Solution

Having the error ellipse in the form of a unit circle simplifies the probability computation considerably because the corresponding two-dimensional probability density function decouples into the product of two identical one-dimensional functions: $p(x, y) = p(x)p(y)$, where $p(x) = \exp(-x^2/2)/\sqrt{(2\pi)}$. The probability density function can be represented as a radially symmetric surface over the circle. The circle is actually the intersection of that surface and a horizontal plane cutting the surface. The total volume under the surface is unity.

In the transformed coordinate system, the extended conflict zone is still in the direction of the (transformed) relative velocity, and the conflict probability is still equal to the portion of the volume under the probability density surface that is within this extended conflict zone. The rotation matrix R in Eq. (18) can be used to rotate the transformed coordinate system about the origin. It can, therefore, be selected so that the relative velocity is in the positive or negative x direction. If

$$\Delta v \equiv v_S - v_R \tag{20}$$

is the relative velocity in the original coordinate system and

$$\Delta \nu \equiv L^{-1}\Delta v \equiv \begin{bmatrix} \Delta \nu_x \\ \Delta \nu_y \end{bmatrix} \tag{21}$$

is the partially transformed relative velocity, then

$$R = \frac{1}{\|\Delta \nu\|}\begin{bmatrix} \Delta \nu_x & \Delta \nu_y \\ -\Delta \nu_y & \Delta \nu_x \end{bmatrix} \tag{22}$$

The boundaries of the extended conflict zone are then the minimum and maximum values of y on the elliptical conflict boundary.

Let Δp_c and $\Delta \rho_c$ represent the original and transformed coordinates, respectively, of points on the conflict boundary relative to the reference aircraft. The equation of the conflict boundary is

$$\|\Delta p_c\| = \|W\Delta \rho_c\| = s_c \tag{23}$$

where s_c is the conflict separation distance (5 n miles) and W is defined in Eq. (13). This equation can be squared and then expanded according to

$$\Delta \rho_c \equiv \begin{bmatrix} \Delta x_c \\ \Delta y_c \end{bmatrix}, \qquad W^T W \equiv \begin{bmatrix} a & b \\ b & c \end{bmatrix} \tag{24}$$

The resulting equation for the elliptical conflict boundary is

$$a\Delta x_c^2 + 2b\Delta x_c\Delta y_c + c\Delta y_c^2 = s_c^2 \tag{25}$$

The minimum and maximum values of Δy_c can then be determined by at least two different methods. One method is to consider Eq. (25) as a quadratic equation in Δx_c with coefficients that are functions of Δy_c. The minimum and maximum values of Δy_c can then be determined by setting the discriminant of that quadratic equation to zero and solving for Δy_c. Another method is to differentiate Eq. (25) with respect to Δx_c and solve the equation $\mathrm{d}(\Delta y_c)/\mathrm{d}(\Delta x_c) = 0$, together with Eq. (25). The result is

$$\Delta y_c = \pm s_c\sqrt{\frac{a}{ac - b^2}} \tag{26}$$

at the minimum and maximum points. Note that a is positive and $ac - b^2$ is positive and invariant with respect to rotation for any ellipse,[10] so the argument of the square-root function must also be positive.

The conflict probability is the portion of the volume under the surface of the probability density function that is within the extended conflict zone. Because the probability density function decouples into $p(x, y) = p(x)p(y)$ and the conflict boundaries are parallel to the x axis, the expression for the conflict probability P_c can be simplified as follows:

$$\begin{aligned} P_c &= \int_{-\Delta y - \Delta y_c}^{-\Delta y + \Delta y_c}\int_{-\infty}^{\infty} p(x, y)\,\mathrm{d}x\,\mathrm{d}y \\ &= \int_{-\Delta y - \Delta y_c}^{-\Delta y + \Delta y_c} p(y)\,\mathrm{d}y \int_{-\infty}^{\infty} p(x)\,\mathrm{d}x \\ &= \int_{-\Delta y - \Delta y_c}^{-\Delta y + \Delta y_c} p(y)\,\mathrm{d}y \\ &= P(-\Delta y + \Delta y_c) - P(-\Delta y - \Delta y_c) \end{aligned} \tag{27}$$

where $\Delta y \equiv y_S - y_R$ is the y coordinate of the stochastic aircraft with respect to the reference aircraft and P is the cumulative normal probability function. The latter, defined so that

$$P(z) \equiv \int_{-\infty}^{z} p(s)\,\mathrm{d}s$$

for any random variable z can be determined analytically.[9] This analytical solution for the conflict probability is therefore theoretically exact under the assumptions stated earlier.

The main assumption is that the aircraft velocities are constant (in both magnitude and direction) during the encounter or period of potential conflict. Free-flight trajectories typically will be fairly direct and have few turns, so that assumption is likely to be accurate in most cases. Note that this does not preclude planned turns or other maneuvers before the encounter begins. For constant velocity, the time at which the minimum predicted separation occurs is

$$t_m = t_0 + \frac{\Delta p_0^T \Delta v}{\Delta v^T \Delta v} \tag{28}$$

where Δp_0 is the position difference at time t_0 and Δv is the constant velocity difference, both in terms of Cartesian coordinates. The position difference at minimum separation is then

$$\Delta p_m = \Delta p_0 + (t_m - t_0)\Delta v \tag{29}$$

The minimum separation distance itself is $\|\Delta p_m\|$.

Small variations in aircraft velocity due to wind disturbances or wind-optimal routing have only a small effect in the immediate vicinity of an encounter, so they will not significantly violate the assumption of constant velocity. The predicted velocities at the point of minimum predicted separation are tangent to the flight paths and can be considered first-order linear approximations to the actual trajectories at that point. In the unlikely case that a large heading or speed change is scheduled in the vicinity of a potential conflict, on the other hand, the analytical solution for conflict probability will not be accurate.

Three-Dimensional Case

If the two aircraft are in level flight at different altitudes, or if one or both of the aircraft are climbing or descending, the problem is three dimensional. The basic modifications required to the two-dimensional case are discussed in this section. For simplicity, the along-track axis is defined as the projection of the predicted velocity vector on a horizontal plane. The along-track and cross-track axes are therefore horizontal by definition, and the prediction error ellipsoid is modeled as having its principal axes in the along-track, cross-track, and vertical directions. For en-route flight, the conflict zone is a cylinder or disk with a horizontal radius of 5 n miles and a vertical thickness of 4000 ft.

A coordinate transformation can be used to transform the error ellipsoid into a unit sphere. Most of the preceding analysis still applies but in three dimensions rather than two. The transformation can be decoupled into a two-dimensional horizontal transformation identical to the one discussed earlier and a vertical transformation that is a simple scaling. The conflict zone, which is a circular cylinder in the original coordinate system, is an elliptical cylinder in the

transformed coordinate system. The transformation can still be selected so that the relative velocity is in the positive or negative x direction.

Consider first the case in which both aircraft are in level flight but at different altitudes. In this case, the relative velocity vector is horizontal, and the projection of the disk-shaped conflict zone along the direction of relative velocity forms a rectangular volume. The conflict probability is the product of two cumulative normal probability differences, one that is identical to Eq. (27) and another of the same form that applies to the vertical axis. That is, the horizontal conflict probability of Eq. (27) can be generalized to three dimensions by multiplying it by a vertical conflict probability factor. The vertical factor is $P(-\Delta z + \Delta z_c) - P(-\Delta z - \Delta z_c)$, where Δz is the predicted vertical separation between the two aircraft and Δz_c is the minimum allowed vertical separation (2000 ft), both normalized (divided) by the vertical rms error.

A typical vertical rms error, which is caused primarily by baroaltimeter error, is approximately 100 ft. For all practical purposes, it can be assumed that the vertical error will not exceed ± 400 ft for each aircraft or $\sqrt{2} \times 400 \approx 600$ ft for the altitude difference of two aircraft. Therefore, if the predicted vertical separation is less than about $2000 - 600 = 1400$ ft, the vertical factor is virtually unity, and the three-dimensional conflict probability is essentially equal to the horizontal conflict probability. If the predicted vertical separation is greater than about $2000 + 600 = 2600$ ft, on the other hand, the vertical factor is virtually zero, and the horizontal conflict probability need not even be computed. For a vertical rms error of 100 ft, therefore, the vertical factor needs to be computed only if the predicted vertical separation is between about 1400 and 2600 ft.

The case in which one or both of the aircraft are climbing or descending is more complicated, unfortunately, because the relative velocity is not horizontal, and the projection of the disk-shaped conflict zone along the direction of relative velocity does not form a rectangular volume. The cross section of that volume is a rectangle with halves of an ellipse attached to the top and bottom. Numerical integration can be used to approximate the conflict probability, if necessary, or some heuristic approximation may be possible, but that approximation is not pursued here.

Application to Conflict Resolution

The ultimate purpose of conflict probability estimation is for use in optimal conflict resolution. The problem of conflict resolution involves deciding when to initiate a resolution maneuver and what maneuver to execute. The conflict probability is an important factor in both decisions. This subsection outlines horizontal conflict resolution methods currently under investigation. Vertical conflict resolution is also discussed briefly.

The optimal time to initiate a conflict resolution maneuver is a tradeoff between efficiency and certainty. The farther in advance a maneuver is initiated, the more efficient it is likely to be in terms of extra distance flown, but the less certain will be exactly what maneuver is required or whether a maneuver is required at all. The later a maneuver is initiated, on the other hand, the more certain will be exactly what maneuver is required, but the less efficient and more harsh the maneuver is likely to be. The optimal time to initiate a maneuver can be determined by minimizing a cost function that reflects the statistically expected cost of maneuvering (or not maneuvering) as a function of time. That cost function depends on the conflict probability, the operating cost per unit of distance traveled, and various other issues such as passenger comfort and controller workload.

A conflict is resolved in the horizontal plane by moving the extended conflict zone sufficiently far away from the center of the error ellipse or circle to reduce the conflict probability to some desired level. The resolution maneuver involves changing the direction of the relative velocity for some period of time, as illustrated in Fig. 4. The magnitude of the relative velocity is essentially irrelevant. It is assumed that the aircraft will complete the dynamic or accelerating portion of the maneuver and reach a constant velocity before the encounter (period of potential conflict). The velocity changes can, therefore, be modeled as instantaneous until the static maneuver is determined; the dynamic transients can then be properly accounted for.

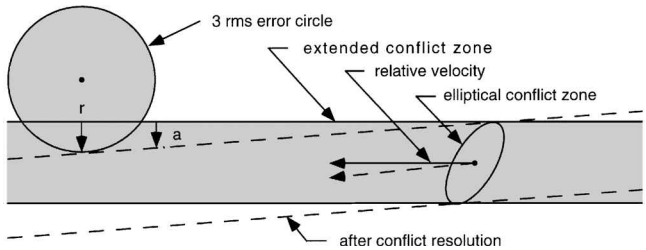

Fig. 4 Conflict resolution geometry in transformed coordinate system.

The key parameters are the time at which the maneuver is initiated, the time at which it is completed, and the angular change of the relative velocity. If the maneuver is completed after the encounter, as shown in Fig. 4, its effect is to rotate the extended conflict zone by angle a about the point at which the maneuver is initiated. If it is completed before the encounter, on the other hand, and the aircraft return to their original velocities, its effect is to translate the extended conflict zone by distance r perpendicular to the relative velocity.

The direction of the relative velocity after resolution can be easily transformed back to the original coordinate system. Then, changes in the individual aircraft velocities must be determined to realize that relative velocity. In general, the change in relative velocity can involve changes in both the magnitude and the direction of the individual velocities. The solution is underdetermined, however, and additional constraints can be applied to simplify the maneuver. For example, the solution can be constrained to require only one aircraft to maneuver. In addition, the maneuver can be further constrained to consist of only a heading change at constant speed or a speed change at constant heading, if desired.

This discussion applies mainly to horizontal conflict resolution, but vertical conflict resolution is also very important for two reasons. First, because the minimum required separation is about 15 times less in the vertical axis than it is in the horizontal plane, vertical conflict resolution may be more efficient in many cases, particularly when the minimum predicted horizontal separation is small or the vertical separation is already almost large enough to avoid a conflict. Second, because vertical conflict resolution is much simpler, it may be appropriate for conflicts involving three or more aircraft. For those cases, determination of efficient horizontal resolution maneuvers can be mathematically complicated and computationally intensive, and accurate and reliable execution can be operationally difficult. Separating the aircraft by altitude, on the other hand, is much simpler.

Validation

The Gaussian statistical model on which the conflict probability algorithm is based was determined empirically by analyzing actual air traffic data.[8] A Monte Carlo simulation was used to validate the algorithm itself. In the Monte Carlo simulation, combinations of path-crossing angles, minimum predicted separations, and times to minimum predicted separation were generated. For each combination, the conflict probability was computed and nominal trajectories were generated. Then the nominal trajectories were perturbed by a series of random prediction errors, each consisting of constant cross-track position error and constant along-track velocity error. These randomly generated errors had the same expected statistics as were used in the conflict probability algorithm: 1 n mile rms cross-track error and 0.25 n mile/min rms along-track error growth rate. Wind-error cross-correlation was not modeled. The empirical fraction of cases in which conflicts resulted was compared with the computed conflict probability.

Table 1 shows a representative sampling of the differences between the computed conflict probabilities and the Monte Carlo simulation results. One million Monte Carlo samples were run for each entry in the table, and each entry corresponds to a particular encounter geometry. The algorithm matches well with the simulation results. The largest magnitude of the difference for all cases shown is 1.8%, and only 5 of the 72 differences in the table are at or above 1% in magnitude. Most of the differences are well below 1% in magnitude, and many are at about 0.1%. Given the accuracy of the underlying error model and the requirements of the application, this

result is more than adequate. A worst-case accuracy of perhaps 5% would have been considered adequate.

The differences are larger than would be statistically expected, however. The expected standard deviation for each table entry is $\sqrt{[P_c(1 - P_c)/N]}$, where N is the number of samples and P_c is the conflict probability. Note that $P_c(1 - P_c) = 0$ if $P_c = 0$ or $P_c = 1$, and the maximum of $\sqrt{[P_c(1 - P_c)]}$ is 0.5 when $P_c = 0.5$. Thus, the maximum expected standard deviation for any table entry cannot exceed 0.0005. One reason that the differences are larger than expected is that the analytical solution is based on the assumption that the prediction error covariance is constant during the encounter, whereas it actually grows with prediction time.

Aircraft pairs with small path-crossing angles tend to have encounters of longer duration, so the assumption of constant covariance during the encounter is likely to be less accurate. This could explain the slightly larger differences in Table 1 for small path-crossing angles. Recall also that aircraft pairs with small path-crossing angles have more wind-error cross-correlation, which is not modeled in this simulation. Although cross-correlation can be exactly accounted for in the conflict probability algorithm, a model of the actual physical phenomenon needs to be developed so that values can be determined for Eq. (11). The conflict probability estimates are, therefore, likely to be less accurate for pairs of aircraft flying in the same or nearly the same direction, but that will improve as wind-error cross-correlation is better understood.

Table 1 Monte Carlo simulation results: computed minus empirical conflict probability based on 1,000,000 samples per entry

Path-crossing angle, deg	Minimum predicted separation, n mile	Time to min separation, min			
		4	8	12	24
15	0	+0.000	−0.009	−0.006	−0.002
15	5	−0.018	−0.003	−0.003	−0.002
15	10	−0.001	−0.006	−0.005	−0.003
30	0	+0.001	+0.006	+0.005	+0.001
30	5	−0.011	−0.004	−0.001	+0.000
30	10	−0.000	−0.004	−0.004	−0.001
45	0	+0.002	+0.012	+0.010	+0.003
45	5	−0.006	−0.003	−0.000	+0.002
45	10	−0.001	−0.006	−0.006	−0.001
90	0	−0.000	−0.000	+0.000	+0.001
90	5	−0.001	−0.001	−0.000	−0.000
90	10	−0.000	−0.000	−0.000	+0.000
135	0	−0.000	−0.003	−0.008	−0.012
135	5	+0.001	−0.001	+0.000	−0.000
135	10	+0.000	+0.001	+0.004	+0.006
180	0	+0.000	+0.000	+0.000	+0.000
180	5	−0.000	−0.000	+0.000	−0.001
180	10	−0.000	−0.000	−0.000	−0.000

Numerical Examples

A set of numerical examples of conflict probabilities and related quantities were generated as a function of encounter geometry. The aircraft speeds were 8 n miles/min (480 kn) in every case, a typical speed for commercial transport aircraft. The conflict separation distance was 5 n miles, the currently used value for en-route airspace. The cross-track rms error was 1 n mile, and the along-track rms error started at zero and grew linearly at a rate of 0.25 n mile/min unless otherwise stated. These values are typical for cruise. (This linear-growth model is typical but is not assumed or required by the algorithm.) Wind-error cross-correlation between aircraft was not modeled.

Figure 5 shows the cumulative separation probability, with prediction time as a parameter, where the path-crossing angle is 90 deg, and the minimum predicted separation is 0 n mile (an exact collision). This value is the probability that the minimum separation will be less than the abscissa value. Figure 6 shows the corresponding probability density (the derivative, with respect to minimum separation, of the cumulative separation probability shown in Fig. 5, determined by numerical differentiation). This plot shows how the density function spreads out as prediction time increases.

It is interesting to see how the expected value of the minimum separation compares with the predicted value as prediction time increases. The predicted value is based on a deterministic trajectory model, with no consideration for trajectory-prediction errors. The expected or mean value, on the other hand, is derived from the cumulative separation probability function P or the separation probability density function p according to

$$E(s) = \int_0^\infty [1 - P(x)]\,dx = \int_0^\infty xp(x)\,dx$$

Figure 7 shows the expected value of minimum separation as a function of time to minimum predicted separation, with minimum predicted separation as a parameter, where the path-crossing angle is 90 deg. The expected separation diverges from the predicted separation, but the group of curves shown converge to a common asymptote for large prediction times. Note that the 0-n mile case does not intersect the origin because the cross-track rms error is nonzero at time zero.

Figure 8 shows the effect of minimum predicted separation on conflict probability. Conflict probability is plotted as a function of the time to minimum predicted separation, with the minimum predicted separation as a parameter, where the path-crossing angle is 90 deg. For small prediction times, the covariances are small, and

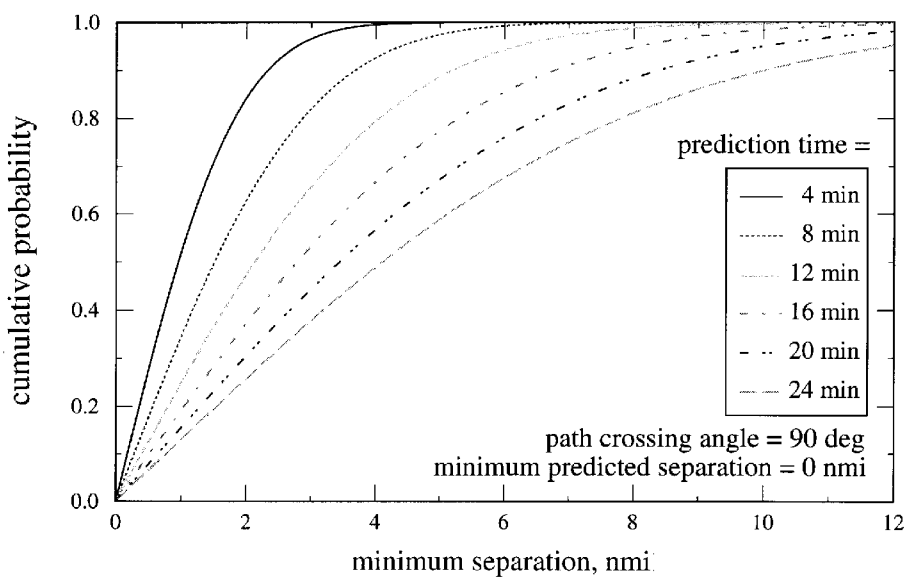

Fig. 5 Cumulative separation probability.

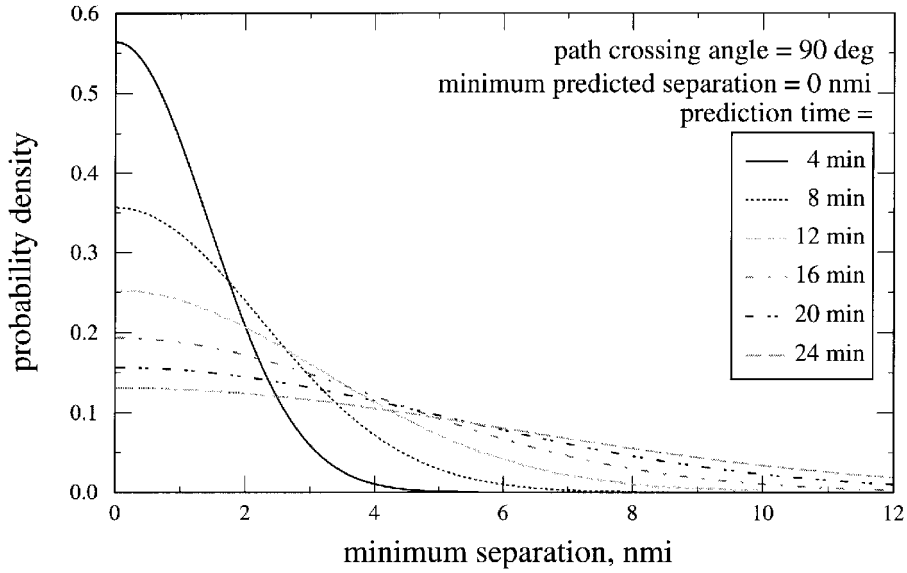

Fig. 6 Separation probability density.

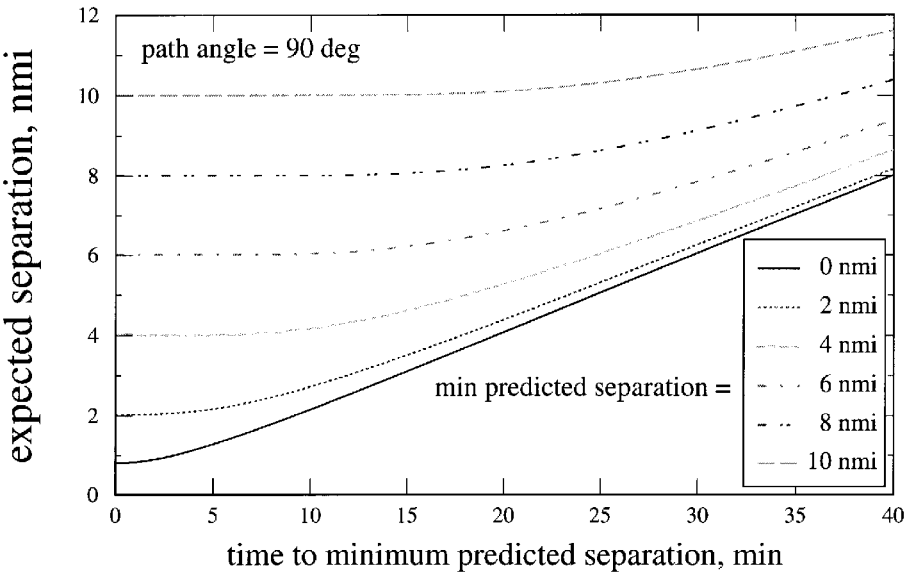

Fig. 7 Expected value of minimum separation.

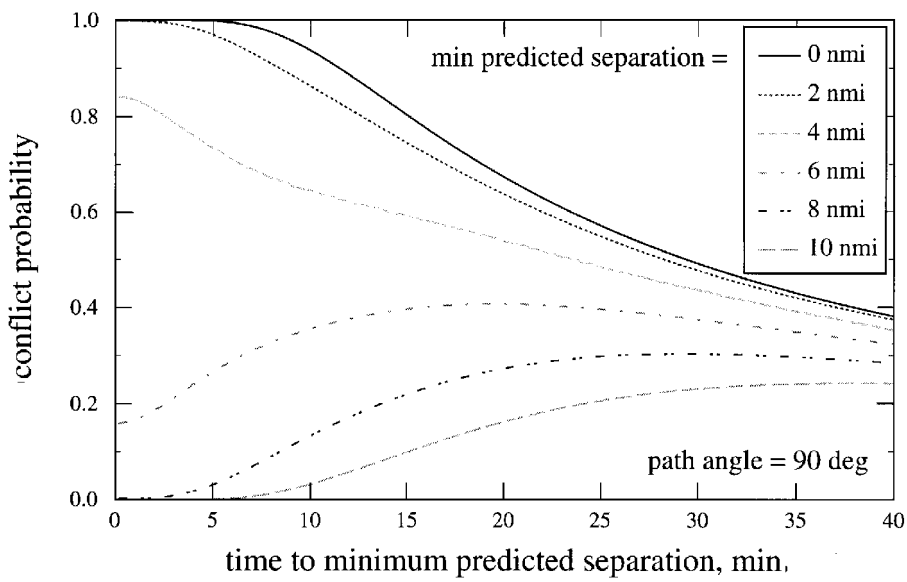

Fig. 8 Effect of minimum predicted separation.

the conflict probabilities are a strong function of minimum predicted separation. For larger prediction times, the covariances grow and the conflict probability becomes a weaker function of the minimum predicted separation. The conflict probabilities converge and asymptotically approach zero as prediction time increases.

Figure 9 shows the effect of path-crossing angle on conflict probability. Conflict probability is plotted again as a function of the time to minimum predicted separation but with the path-crossing angle as a parameter, where the predicted minimum separation is 0 n mile. As a point of reference, the curve for the path-crossing angle of 90 deg is a repeat of the corresponding curve of Fig. 8. As the prediction time increases, the conflict probability decreases faster for smaller path-crossing angles. If wind-error cross correlation were taken into account, however, these curves would be very different for smaller path-crossing angles. A portion of the trajectory-prediction error would cancel in the position difference, and the effective error growth rate would be smaller. Hence, the conflict probabilities for smaller path angles would be higher than those shown in Fig. 9.

Figure 10 shows the effect of prediction-error growth rate on conflict probability. Conflict probability is plotted again as a function of the time to minimum predicted separation but with the along-track rms error growth rate as a parameter. The value of 0.25 n mile/min or 15 kn has been used throughout this paper for the along-track rms error growth rate, but values of 10 and 20 kn are also shown in Fig. 10. For each of the three values of error growth rate, conflict probability is plotted for minimum predicted separations of 0 and 10 n miles. Note that the three pairs of curves could be collapsed into one pair by scaling the horizontal axis by the along-track error growth rate. That is, if the horizontal axis were the along-track error, the three pairs of curves would be identical. Showing them separately does, however, illustrate some important characteristics.

For minimum predicted separations substantially less than the minimum allowed separation, the conflict probability starts at unity and decreases monotonically as a function of prediction time. The effect of larger error growth rates is to cause the conflict probability to decrease more rapidly as a function of prediction time. For minimum predicted separations substantially greater than the minimum allowed separation, on the other hand, the conflict probability starts at zero, increases to some maximum value, and then decreases back toward zero. This phenomenon occurs because the individual error ellipses expand and start to overlap, but then after the maximum conflict probability they expand even more and the probability density function becomes flatter. The effect of larger error growth rates is to cause the conflict probability to initially increase more rapidly as a function of prediction time and then to decrease more rapidly after the maximum.

Finally, because computational efficiency is a major concern in a real-time air traffic control system, basic timing tests were

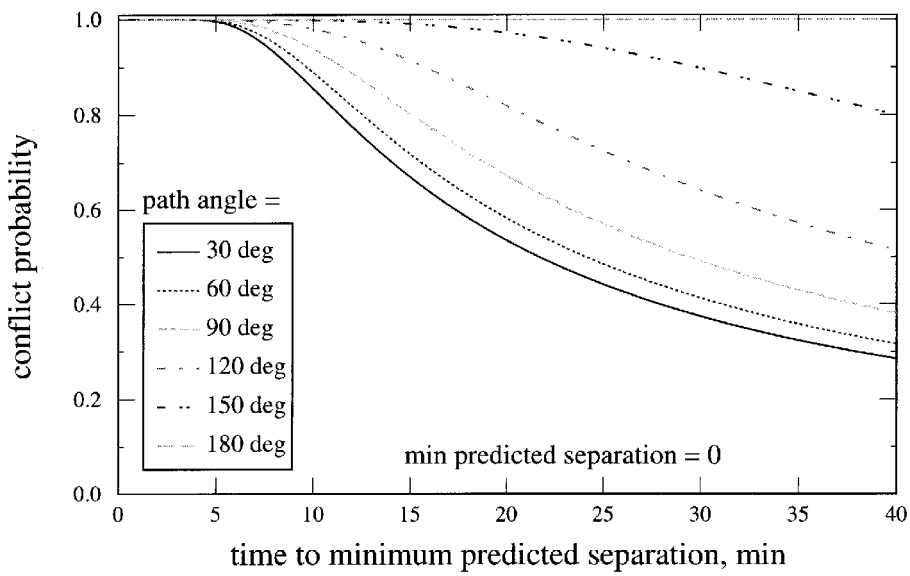

Fig. 9 Effect of path-crossing angle.

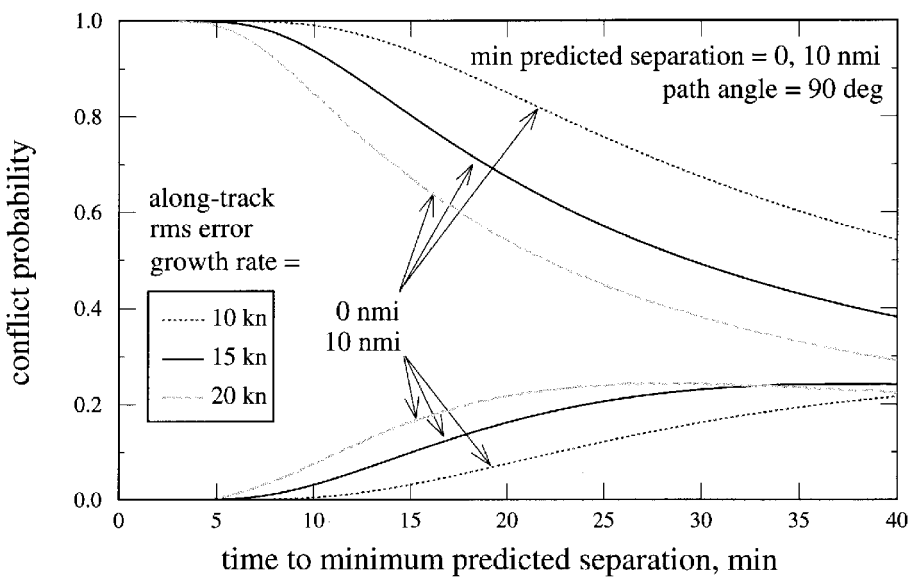

Fig. 10 Effect of prediction error growth rate.

performed on the conflict probability algorithm running on a Sun SPARC 10 workstation. These tests were for the conflict probability algorithm only and did not include trajectory prediction, wind-error modeling, or any other part of the problem. The average computation time per aircraft pair was slightly under 0.6 ms. In addition to being theoretically exact under the stated assumptions, this time is approximately two to four orders of magnitude faster than a numerical solution, depending on the method and level of resolution of the numerical integration. Furthermore, it is fast enough to be used directly in a real-time system.

Conclusion

A method has been developed to accurately and efficiently estimate the probability of conflict for aircraft pairs in free flight. The resulting probability estimates are necessary for optimal conflict-resolution, and the analysis behind the estimates is useful for developing an optimal conflict-resolution algorithm. Some significant aspects of the problem still need to be addressed, such as an efficient approximation for ascending and descending aircraft and a wind-error cross-correlation model. Although some heuristic methods may be needed to fill these gaps, a sound theoretical and numerical foundation has been established. The algorithms and software developed for this study soon will be incorporated into a conflict prediction system and tested on real air traffic data. This work will eventually help air traffic controllers maintain safe and efficient free flight.

References

[1] Anon., Air Traffic Control Federal Aviation Administration Order 7110.65, U.S. Government Printing Office, Washington, DC.

[2] Anon., Final Report of the RTCA Task Force 3, Free Flight Implementation, RTCA, Inc., Washington, DC, Oct. 1995.

[3] Anon., "Free-For-All Flights," *Scientific American*, Vol. 273, No. 6, 1995, pp. 34–37.

[4] Phillips, E. H., "Free Flight Poses Multiple Challenges," *Aviation Week and Space Technology*, Vol. 144, No. 13, 1996, p. 27.

[5] Benjamin, S. G., Brundage, K. J., and Morone, L. L., "The Rapic Update Cycle, Part I: Analysis/Model Description," *Technical Proceedings Bulletin*, No. 416, National Oceanic and Atmospheric Administration/National Weather Service, Washington, DC, 1994.

[6] Devenyi, D., and Schlatter, T. W., "Statistical Properties of Three-Hour Prediction 'Errors' Derived from the Mesoscale Analysis and Prediction System," *Monthly Weather Review*, Vol. 122, June 1994, pp. 1263–1280.

[7] Erzberger, H., and Nedell, W., "Design of Automated System for Management of Arrival Traffic," NASA TM-102201, June 1989.

[8] Ballin, M. G., and Erzberger, H., "An Analysis of Landing Rates and Separations at Dallas/Ft. Worth Airport," NASA TM-110397, July 1996.

[9] Press, W. H., Tuekolsky, S. A., Vetterling, W. T., and Flannery, B. P., *Numerical Recipes in C: The Art of Scientific Computing*, Cambridge Univ. Press, New York, 1992.

[10] Thomas, G. B., and Finney, R. L., *Calculus and Analytic Geometry*, 5th ed., Addison–Wesley, Reading, MA, 1979.